Visualization of Regular Maps: The Chase Continues

Jarke J. van Wijk, *Member, IEEE*

Abstract—A regular map is a symmetric tiling of a closed surface, in the sense that all faces, vertices, and edges are topologically indistinguishable. Platonic solids are prime examples, but also for surfaces with higher genus such regular maps exist. We present a new method to visualize regular maps. Space models are produced by matching regular maps with target shapes in the hyperbolic plane. The approach is an extension of our earlier work. Here a wider variety of target shapes is considered, obtained by duplicating spherical and toroidal regular maps, merging triangles, punching holes, and gluing the edges. The method produces about 45 new examples, including the genus 7 Hurwitz surface.

Index Terms—regular maps, tiling, tessellation, surface topology, mathematical visualization

1 Introduction

In graph theory, a map is a crossing-free embedding of a graph on a surface. A regular map is a map that is vertex-, face-, and edge-transitive, *i.e.*, each vertex, face, and edge is topologically indistinguishable from the other elements of the same type. Classic examples of regular maps are the Platonic solids, which are regular maps on spheres. But also for surfaces with higher genus g such regular maps can be found. The genus is informally equal to the number of holes in the shape. The Euler number $\chi = V - E + F$, with V the number of vertices, E the number of edges, and F the number of faces is an invariant for the genus of the surface, and for orientable surfaces $\chi = 2 - 2g$.

Regular maps on tori, genus 1 surfaces, can be found easily. As an example, folding a chessboard by matching opposite sides gives a torus decorated with a regular map. For genus 2 and higher, the problem to produce visualizations of regular maps is much more complex. It is known what regular maps exist. Conder [4] has enumerated all reflexible regular maps on orientable surfaces up to genus 101, and found 6104 different cases. Each map is described here via its symmetry group. In graphics terminology, the structure of the faces, edges, and vertices is given, but no possible geometric realization, *i.e.*, no possible space models are given.

It is a fascinating problem to produce space models of regular maps: surfaces embedded in 3D, decorated with colored faces, edges, and vertices depicting regular maps. Regular maps are not an esoteric, abstract concept, they can be described in a very concrete and geometric way. For instance, the Hurwitz genus 7 surface consists of 168 triangles, at each vertex 7 triangles meet, and each Petrie-polygon (a closed zig-zag path over the edges) has 18 edges. But, what could such a shape look like? The papers of Carlo Séquin [20, 21, 22] give an interesting and entertaining account on how to attack this problem; we argued earlier [24] that this class of puzzles is close to perfect.

Also, the scope of this topic is large. Regular maps relate to many different branches of mathematics [14]. Symmetry is described by algebra, shapes by geometry, and regular maps can be studied from the point of view of surface topology, combinatorial group theory, graph theory, hyperbolic geometry, and algebraic geometry. Finally, there is an artistic interest, as these highly symmetric objects lead to complex and fascinating shapes.

Roughly, there are two main approaches to come up with solutions for the visualization of regular maps. The work of Séquin is the key example of the manual approach. He has produced a steadily growing set of space models of regular maps by attacking them one by one, using a combination of heuristics, insights, and a variety of media, ranging from sketches to computer models to 3D printing. An alternative is to use an automatic approach. In 2009 we translated the problem into automatically finding matching patterns in hyperbolic space. About 50 new solutions resulted, but for many regular maps it is still unknown what their space models could look like.

The choice of the target surface is important, both in manual and automatic approaches. Typically a smooth closed surface is used, covered with a face-transitive map. Decorating each face with the same pattern should hopefully lead to a depiction of a regular map. Séquin used a *tetrus*, the shape that results when replacing the edges of a tetrahedron by tubes, to visualize regular maps of genus 3. We extended this approach, and used tubified regular maps as target surfaces, where quarter tubes were used as target faces.

In this paper we present a generalization of our earlier approach. We use a richer set of target surfaces, obtained by duplicating space models of regular maps of genus 0 and 1, merging triangles, systematically punching holes, and gluing the edges. This leads to a face-transitive map, consisting of topologically identical faces, configured in a certain pattern, and which may have vertices of different valences around their perimeter. Also, regular maps can be simplified to face-transitive maps. This approach is more generic than the earlier approach, which was limited to the use of tubified regular maps as target shapes.

Like in the earlier approach, we use a two-step matching process to find new solutions. First, simplified regular maps and target surfaces are matched, to find combinations of these with similar faces and similar patterns; next, exact solutions are sought for by aligning points of the target surface with points of the regular map in hyperbolic space. A novelty here is the smoothing of meshes in hyperbolic space, leading to edges with less kinks.

Compared to the earlier approach, the number of regular maps that can be visualized almost doubles, and all examples given in this paper are new. Specifically interesting is the first visualization of the Hurwitz genus 7 surface, also known as the MacBeath surface.

In the next section we give a short introduction on concepts used, and discuss related work. Next, we give a global overview of our approach in Section 3, followed by a detailed description of the various steps in Sections 4 to 7. Results are presented and discussed in Section 8, followed by conclusions in Section 9.

2 Background

As mentioned, regular maps are located at the intersection of different branches of mathematics, and to understand and process regular maps, some background is needed. We assume basic knowledge of group theory and hyperbolic geometry. We used Beardon [2], Katok [12], and Anderson [1] for understanding tilings, Fuchsian groups, and hyperbolic geometry; Firby and Gardiner [9] for surface topology; Coxeter [6], Coxeter and Moser [7] and Conder and Dobcsányi [5] for regular maps. Here we describe some basic concepts and terminology, mainly by examples, that are used in the following sections.

• *Jarke J. van Wijk is with Eindhoven University of Technology. E-mail: j.j.v.wijk@tue.nl.*

Manuscript received 31 Mar. 2014; accepted 1 Aug. 2014. Date of publication 11 Aug. 2014; date of current version 9 Nov. 2014.
For information on obtaining reprints of this article, please send e-mail to: tvcg@computer.org.
Digital Object Identifier 10.1109/TVCG.2014.2352952

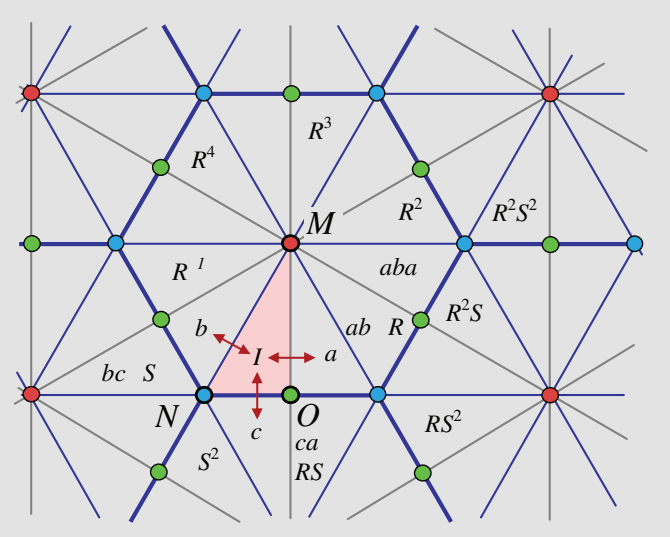

Fig. 1. A triangular tiling is produced by reflecting a triangle MNO over its edges, using reflections a, b, and c. The corresponding group is the triangular group. Here $T(6,3,2)$ is shown, and the vertices M,N, and O are of order 6, 3, and 2. The original vertices and their copies can be partitioned into three fixed point sets, indicated by the color of the vertices.

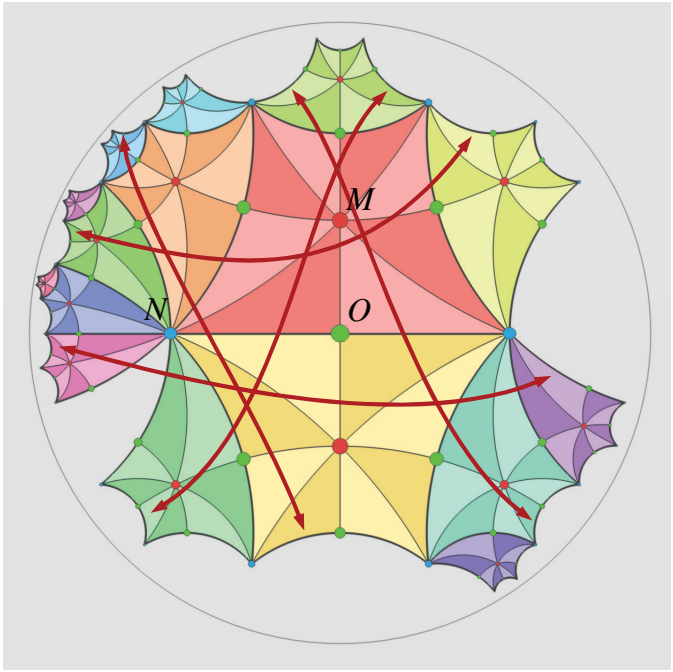

Fig. 2. Plane model of a regular map: R5.6 of {4,8} type. The group of R5.6 is obtained by adding for instance the relator $(abc)^8$ to T(4, 8, 2). Some pairings of edges are indicated with arrows, a space model is obtained when the surface is lifted to 3D and paired edges are glued. The crossings of the arrows indicate that this closed surface is not a sphere, and indeed, a genus 5 surface is required. Unique colors are used to show the faces of the regular map, the triangles of the associated triangle group are shown using a light-dark modulation.

2.1 Triangular tilings

We first consider triangular tilings. Consider a triangle MNO with angles π/p, π/q, and π/r, and let a, b, and c denote reflections on the edges (see Figure 1). If we repeatedly apply these reflections, the plane is covered by triangles. The triangle is a *fundamental region*. If we limit ourselves to orientation preserving transformations, we can use the rotations $R = ab$, $S = bc$, and RS around the points M, N, and O. These points are *elliptic fixed points* of *order* p, q, and r. As a result of the repeated rotations, multiple copies of M, N, and O are produced, so called *conjugate* or *congruent points*. We call the points M, N, and O *base points*, and a set consisting of a base point and its conjugate points a *fixed point set*. If only rotations are used, pairs of neighboring triangles can be used as fundamental regions.

In terms of combinatorial group theory, the abstract presentation of the corresponding triangle group is

$$T(p,q,r) =< a,b,c \,|\, a^2 = b^2 = c^2 = (ab)^p = (bc)^q = (ca)^r = I >,$$

where a, b, and c are the *generators*, and the following terms are *relators*. Elements of the group are produced by concatenating generators to *words*, which can be simplified by removing subwords that are equal to relators. Here, $a^2 = aa = I$ denotes that applying a twice leads to the original result, the term $(ab)^p$ denotes that applying the rotation ab p times also leads to identity. In representation theory, group elements are represented as matrices, and the group operation is matrix multiplication. Here, the elements denote isometric transformations of either the sphere, the Euclidean plane, or the hyperbolic plane, represented as 3D transformation matrices, 2D homogenous transformations, or Möbius transformations, using the Poincaré disk model for the hyperbolic plane.

2.2 Regular maps

Regular polygon tilings can be defined using triangle groups $T(p,q,2)$, *i.e.*, using right-angled triangles. If we join all triangles around vertices M, we obtain p-sided polygons, and at all vertices q polygons meet. This is denoted as a $\{p,q\}$ tiling using the Schläffli symbol. R denotes a rotation of a polygon around its center M, and S a rotation around a vertex N. R and S are automorphisms of the tiling, as they both map the tiling onto itself. As a result, all faces, edges, and vertices are topologically indistinguishable, and the tiling is face-, edge-, and vertex-transitive. The presentation of the corresponding group of automorphisms is

$$G(p,q) =< R,S \,|\, R^p = S^q = (RS)^2 = I >,$$

where the relator $(RS)^2$ describes a full rotation around the center O of an edge.

The Platonic solids can be described directly using these definitions as tilings of the sphere, *i.e.*, $\{3,3\},\{4,3\},\{3,4\},\{5,3\}$, and $\{3,5\}$. Two other tilings of the sphere are the hosohedron, also known as beachball, described by $\{2,q\}$, and the dihedron, given by $\{p,2\}$.

The tilings $\{4,4\},\{3,6\}$, and $\{6,3\}$ cover the plane with squares, triangles, and hexagons. To obtain a regular map on a torus, we cut out a part of the tiling and match opposite sides. The corresponding group is a quotient group of the original group, obtained by adding a relator. Taking the chessboard as an example again, the transformation RS^{-1} translates a square one step to the right, hence a group G(4,4) with $(RS^{-1})^8$ as additional relator represents a torus covered with 64 squares.

Tilings with $2p+2q-pq<0$ cover the hyperbolic plane. As long as this constraint is satisfied, arbitrary values for p and q can be used, in contrast to the sphere and the plane, which permit only a limited set. Such tesselations can be conveniently depicted using the Poincaré disk model. Also here regular maps can be derived by cutting out a part of the tesselation and matching edges at the boundary, leading to a closed surface of genus 2 or higher. Again, the associated group is obtained by adding relators. This is illustrated in Figure 2, showing a plane model of a regular map. Such a plane model can easily be derived from the definition of a group, but to fold up this model to a space model that shows symmetries of the map is far from trivial, and the primary challenge discussed in this article.

Conder and Dobcsány [5] have enumerated all regular maps of genus 2 to 15 on orientable surfaces with a computational group theory

approach, using exhaustive search, optimized software, smart heuristics, and hundreds of hours of computer time, later Conder has enumerated all regular maps up to genus 101 [4]. In their lists reflexible regular maps are denoted with a label R$g.i$, where g is the genus of the surface and i an index. They do not list dual maps (where vertices and faces swap roles) separately, we use a prime to indicate that we consider dual maps. For each map a set of additional relators is given. His list of reflexible regular maps on orientable surfaces contains 6104 entries, counting dual maps separately. The description in terms of generators and relators precisely describes the topological structure, and can be used to visualize the regular map as a plane model in the hyperbolic plane. Figure 2 shows a plane model of regular map R5.6, which we use as running example. But, no information is given how such a plane model can be mapped nicely on a closed surface embedded in 3D, leaving this as a challenge for the graphics, visualization, and mathematical art communities.

2.3 Space Models of Regular maps

Depictions of Platonic solids are literally classic, but space models of regular maps on surfaces with genus 2 and higher have only been studied more recently. Klein's regular map, also known as the Hurwitz surface of genus 3, consists of 56 triangles with 24 vertices where seven triangles meet. Such a $\{3,7\}$ tiling is special, as Hurwitz [11] has proven that for these tilings the maximal number of $84(g-1)$ symmetries is obtained for a surface with genus g. Schulte and Wills [19] found a polyhedral version of this regular map in 1985; and more examples of polyhedral models have been found, see for instance [3, 8, 18]. Helaman Ferguson's sculpture *The Eightfold Way*, 1993, at MSRI in Berkeley [13] visualizes Klein's map on a thickened and smoothed tetrahedral wireframe, in white Carrara marble.

Séquin [20] took inspiration from this work, and presented more examples of regular maps, such as a $\{4,5\}$ map on a genus 4 surface [21], and space models of (among others) R2.4, R2.5, R3.11, R5.10, and R5.11. His papers are inspiring for people that want to attack this problem by hand, and vividly show how a rich set of media can be used for analysis and presentation.

In 2009, we presented an automatic approach to visualize regular maps [24]. The method is based on finding a match between a regular map and a target surface in hyperbolic space. To obtain target surfaces, space models of regular maps were used as starting point, and the edges were replaced by tubes, where each tube is modeled with four symmetric faces. Next, these faces were aligned with the regular map in hyperbolic space, by selecting points of the regular map as corner points of one face such that symmetries were satisfied. Next, the pattern of the regular map was projected to the target surface, based on this alignment. To construct target surfaces, not only space models of genus 0 and 1 regular maps were used, but also space models of higher genus regular maps that resulted from applying the method. This recursion gives rise to highly intricate and complex, but still highly symmetric target surfaces.

Razafindrazaka [16] has shown how aesthetically more pleasing results can be obtained by applying a force-directed method on the edges before they are tubified; another recent result is a new and highly symmetric space model for R13.2 [17].

Our earlier method produced about 50 new models, but also, many regular maps escaped, as no match could be found. Here we extend his method by using a richer collection of target surfaces and allowing for more complex faces besides quarter tubes.

3 Approach

For a high level description of our approach, we start with a much simpler problem: the visualization of cyclic groups, using a practical case. Suppose that we have the task to mark 18 intervals on a clock, which has 12 marks for 5 minute intervals. We observe that 18 and 12 have 6 as greatest common divisor, and that we can decompose the 18 intervals into 6 sets of three intervals, and 12 into 6 sets of two intervals. We can visualize this along a line, and see that each set of three given intervals has to be matched to two intervals on the clock. We map this pattern of three intervals to 10 minute intervals on the clock, and we are done. More technically, we decompose the cyclic group C_{18} into $C_6 \times C_3$, the target into $C_6 \times C_2$, and align the patterns within each element of the two C_6 groups.

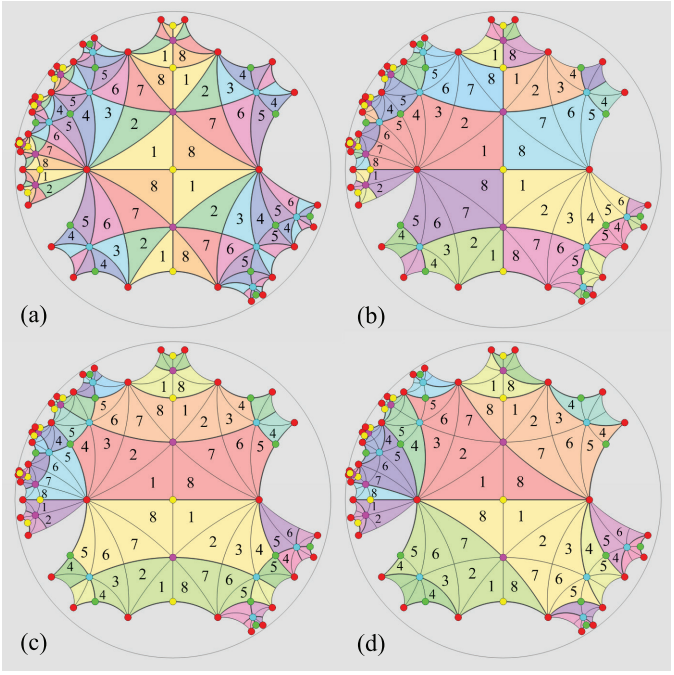

Fig. 3. Factorization HA of R5.6, with $H = C_2 \times D_8$, where D_8 is the dihedral group with 8 elements. H is generated by rotations over π around the points M, N, and O. (a) All triangles $Ha_i, a_i \in A, i = 1,\ldots,8$ are labeled and colored according to their label; (b), (c), and (d) show some possible choices for A, giving different fundamental regions: sets of triangles with different labels are combined and given unique colors.

Our approach is comparable, but here we have to deal with more complex groups; instead of matching along a line we match on the hyperbolic plane; and we are not constrained to using a circle as target, but have freedom to define target surfaces with a certain structure.

We first discuss how to factorize maps. We systematically merge triangles, and present characterizations of the resulting patterns and faces, such that we can match the overall structure of regular maps and possible target surfaces. Next, we present a new approach to produce surfaces with genus greater than 0, based on duplicating surfaces, merging triangles, punching holes, and gluing the edges. The factorizations of the patterns of the map and the target surface help to find matches, which have to be carefully aligned, as discussed next.

4 Factorization

First we consider how to factorize maps and how to obtain compact representations of these. Suppose that we have a closed surface with a face-transitive tiling with associated group G. This includes regular maps, where G is a quotient group of the triangle group. We can decompose this group as $G = HA$, where H is a subgroup of G and A a subset (not necessarily a group) of G. For an example, see Figure 3. The yellow triangles, labeled with 1, are the elements of H. They are produced by repeated application of a set of generating transformations, here R^2, S^4, and RS (rotations over π over M, N, and O), on the triangle that corresponds with the identity element. As a next step, we take another triangle, not yet colored, assign a new label and color, and again apply the generating transformations. We repeat this until all triangles are labeled and colored. Now, for A we can select arbitrary sets of triangles, as long as all labels are represented and each triangle in A has a different label. To produce nice faces however, we select sets of neighboring triangles and require the boundary to be convex. Specifically, the boundary should be hyperbolically convex: inner angles should be $\leq \pi$, edges should be hyperbolic lines, *i.e.*, circular

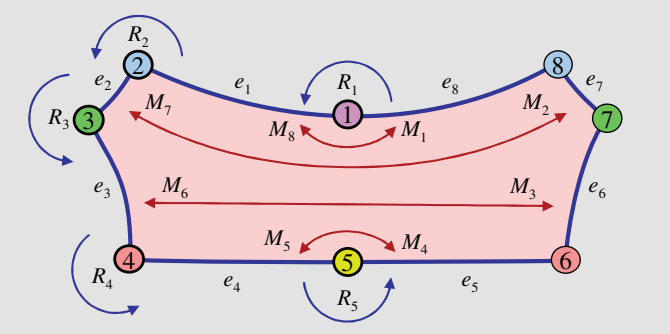

Fig. 4. Example of a fundamental region of a Fuchsian group, based on Figure 3(c). Vertices that belong to the same set of conjugate points are assigned the same color, the first five points are base points. Associated with these are rotations R_i over π, hence all base points are of order 2. Furthermore, pairwise mappings of edges are shown.

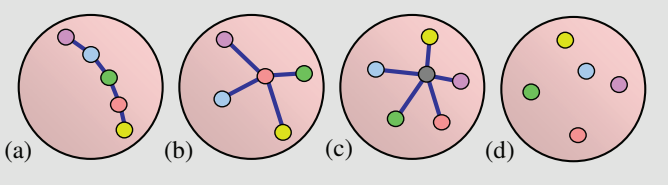

Fig. 5. (a) Folding up the fundamental region of Figure 4 gives a sphere, decorated with vertices and a cut line; (b) similar, for Figure 3(d); (c) standard cuts used for explaining Fuchsian groups, using an extra order 1 vertex; (d) the fundamental region can be characterized by the genus of the surface, and the number of fixed elliptic points and their orders. This is summarized in the Fuchsian signature, here (0; 2, 2, 2, 2, 2).

arcs in the Poincaré disk model. This set of triangles is a fundamental region. By considering each copy of this set as a face, we obtain a face-transitive tiling of the regular map. Multiple choices are possible (see Figure 3), and also choices can be made that do not align with triangle boundaries (see Figure 10).

The group H describes the overall pattern of the faces, next we need to describe the faces themselves in a generic way. For this, the concept of Fuchsian groups [2, 12] is very convenient, here we give an informal introduction. Poincaré has studied face-transitive tilings [15]. In such tilings all edges of a face can be pairwise mapped, and at each vertex the sum of the angles of all incident faces adds up to 2π (see Figure 4). Some vertices are copies of other vertices at the boundary, so-called conjugate points. The number n of different vertices, excluding conjugate points, and their degree of rotational symmetry or order $m_i, i = 1,\ldots,n$, are characteristic for the tiling. Furthermore, because all edges can be mapped to each other, we can turn a single face into a closed surface by gluing corresponding edges, giving a so called *orbifold* (see Figure 5, where the orbifold is a sphere). The genus g of this surface can be larger than 0, and is another characteristic. Taken together, the signature of a Fuchsian group is $(g;m_1,m_2,\ldots,m_n)$, and this gives a compact representation of the tiling, independent of the arbitrary choice of the fundamental region.

Suppose now that we have a regular map with associated group G_S as source, and a possible target surface with matching genus g, which has a face-transitive map with associated group G_T, each of which can be decomposed via $G_S = H_S A_S$ and $G_T = H_T A_T$. A minimal condition for mapping here is that H_S and H_T are equal: both source and target must have the same number of faces, with the same structure. This condition can be trivially satisfied by using $H_S = H_T = I$, but that leaves us the difficult problem how to map the plane model in one step to the target surface. We therefore aim for large common subgroups of G_S and G_T for which the signatures of the Fuchsian groups of the source and target tiling are equal.

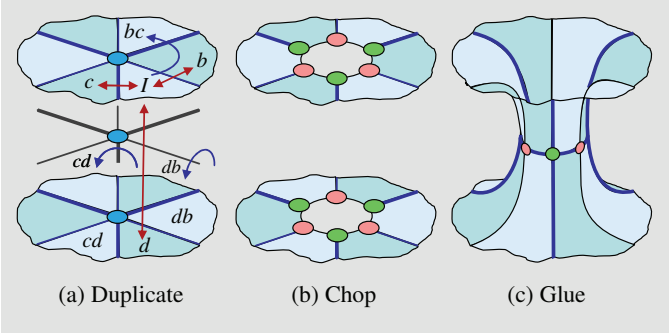

Fig. 6. Basic operations to obtain target surfaces. (a) The original surface is duplicated, giving two copies. A new generator d is introduced, actions like db and cd act as rotations around edges of the original surface. (b) Next, areas around points, here N, are removed and new order 2 rotation points are introduced. (c) The edges of the holes are glued. The original order 3 rotation point is replaced by six new rotation points, in two different classes.

5 Target Surfaces

Earlier, we used tubified wireframes of regular maps. We can also obtain such surfaces as follows (see Figure 6). We duplicate the surface of a regular map, *i.e.*, we form positive and negative offset surfaces above and below the given regular map. Next, we remove the centers of the faces of the regular maps and cut holes in both surfaces. Finally, we glue all edges of pairs of holes, forming connecting tunnels between the two offset surfaces. Thus we obtain again one single closed surface, but with more faces and a higher genus. This inspires us to generalize this process. We extend it in two ways. First, instead of just considering faces of regular maps, we consider face-transitive variations of these, obtained by the process described in the previous section. Second, we allow for punching multiple fixed point sets. One special concern here is the derivation of the corresponding groups. In our earlier work, we derived these manually for tubified wireframes, here we propose a more generic approach.

5.1 Duplicate and Merge

Our starting point is a genus 0 or 1 surface (a sphere or a torus) covered by a regular map. We can easily produce a double walled version by replacing the surface by two copies, one offset to outside, the other offset to the inside. As a result, the number of triangles and the order of the group doubles. To describe the group structure of this double walled version, we introduce a new generator d, besides a, b, and c that generate the triangle group (see Figure 6a). The effect of d is that a triangle is moved from one wall to the other wall. At first, this seems to be a translation, however, it is better characterized as (yet another) reflection. The outside of the triangle becomes the inside, and also, repeating d twice gives identity, *i.e.*, $d^2 = 2$. Next, we consider the effect of combining d with a, b, and c. Figure 6a shows that $(cd)^2 = I$: if we flip a triangle along an edge (c); move it to the other wall (cd); flip it again (cdc); and move back to the original wall ($cdcd$); the triangle is back to its original position. In other words, cd can be considered as a rotation around an edge of the original surface, and the same holds for bd and ad.

A regular map on a sphere can be defined via a triangle group $T(p,q,2)$. The preceding discussion leads to a definition of the group of the new, double walled shape:

$$G_T(p,q,2) = < a,b,c,d \mid a^2 = b^2 = c^2 = d^2 = (ab)^p = (bc)^q = (ca)^2 = (ad)^2 = (bd)^2 = (cd)^2 = I > .$$

For regular maps on tori and on higher genus shapes, the same additional relators as for the original maps have to be added.

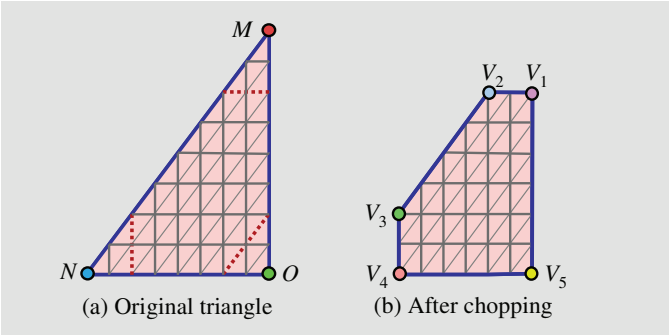

Fig. 7. Mesh used for modeling target surfaces. (a) For each triangle a rectangular mesh is used, on which mesh triangles are defined. A set of possible chop lines is indicated. (b) Mesh after chopping M and N and introducing new fixed points.

The next step is to merge triangles to obtain larger faces and face-transitive maps. In the preceding section we described how to factorize triangulations, and the same procedure can be used here. To keep implementation efforts within bounds, we use the following restrictions on H_T, A_T, and the associated fundamental regions F:

- Copies of F must be congruent without reflections, in other words, only subgroups H_T are used that result from generators with words with an even number of elements a, b, c, and d. One consequence is that F consists of an even number of triangles;
- d should appear in one of the generators of H_T, such that an F can be found that is located on one of the walls only; also, application of d on F should produce a counterpart located directly opposite at the other wall;
- F must be hyperbolically convex;
- The genus g of F must be 0.

We used GAP [10] to derive subgroup lattices of the extended groups for regular maps up to genus 50 and stored these for further processing. Besides descriptions of the subgroup in terms of generators, GAP also provides descriptive names for the groups. These are useful for understanding, and also for fast tests on group equivalence, which is needed for matching H_S and H_T.

Given an appropriate subgroup H_T, finding fundamental regions A_T that meet the requirements for simplicity is fairly straightforward. We used a breadth first search algorithm to enumerate different solutions.

5.2 Chop and Glue

The next step is to turn the double walled object into one closed surface again. First, we determine fixed point sets $P_i, i = 1,\ldots,n$ for the n base points from the fundamental regions found in the preceding step. For each of these sets, we can remove a region around all points in the set, and glue the boundaries of corresponding regions at opposite walls. As a result, we obtain a single closed surface with multiple tunnels between the two offset surfaces. The group structure of this surface is the same as described in the previous section: we do not introduce new faces, remove or add symmetries. However, the genus of the surface and the signature of the Fuchsian group of the covering tiling do change.

The effect of the duplicate operation on the genus of the surface is that the Euler number χ doubles, as the number of vertices, edges, and faces doubles. Furthermore, if two points with s incident edges are chopped and glued, s new vertices and edges are created (which has no effect on χ, as they cancel each other), but also two original points are removed. Hence, if in total k points are chopped, χ decreases with $2k$. Using primes to denote the new values, we find $\chi' = 2\chi - 2k$, and after substitution of $\chi = 2-2g$ we find $g' = 2g+k-1$.

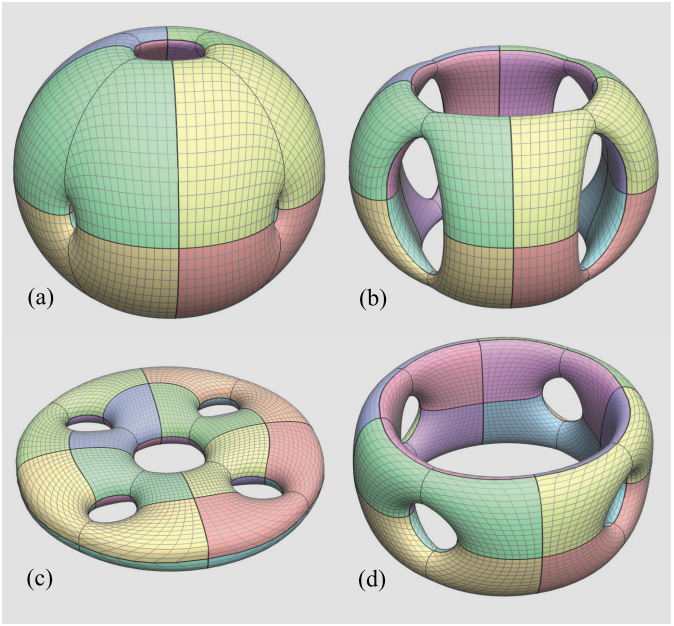

Fig. 8. Examples of different instances of similar target surfaces. The starting point is a duplicated 4-hosohedron, with pairs of triangles merged to faces ($A = \{I, b\}$). Each face is assigned a unique color. (a) The target surface is obtained by duplicating and chopping M and N points. (b) Using larger holes makes the interior better visible. (c) Morphing the surface to a punched disk clearly shows that this is a genus 5 surface. (d) Using a punched ring visualizes the group structure $C_2 \times D_8$ of the faces. The ring can be rotated around the central axis through four steps of $\pi/2$ and through π around a line through two opposite holes (D_8); the wall of the ring can be rotated over π around a circle through the centers of the smaller holes (C_2). Combining these transformations, each face can be mapped to any other of the 15 faces, *i.e.*, the map is face-transitive.

Concerning the Fuchsian signature, the genus of the face after folding up does not change, but the list of orders does. If the original signature was $(g; m_1, m_2, \ldots, m_n)$, the effect of chopping and gluing of the point with order m_j is that it is replaced by two order two rotation points (see Figure 6: the blue order three point is replaced by red and green points of order two). Such a configuration is for instance produced by generators $S = bc$ (rotation around the center vertices) and cd (rotation to the other wall around the edge matching with reflection c on the original surface). After chopping and gluing, six new vertices are inserted on the incident edges. Each of these vertices has order two, and they form two sets of conjugate points. The two base points of these sets correspond to the rotations cd and db.

Multiple fixed point sets can be dealt with in this way, giving a variety of face transitive maps on surfaces with varying genus. The simple effect of removing rotational points on the genus of the surface and the Fuchsian signature can be used to quickly generate alternative compact descriptions of these target surfaces, which can be used to find a match with the set of regular maps to be visualized.

5.3 Embedding in 3D

Geometric modeling of the surfaces in 3D is straightforward. We use grids with a rectangular structure for the triangles covering the spheres and tori (Figure 7). Offsetting is done using the normals on the surface, chopping base points is done by removing a user defined number of strips from the corners. In our implementation, this number was taken to be the same for all corners. As a result, when only one point is chopped, a large number of strips can be removed, leading to images similar to the earlier tube-images. However, if multiple points are chopped, the number of strips that can be removed is limited by intersecting chop lines. This is not a problem if a depiction as holes is

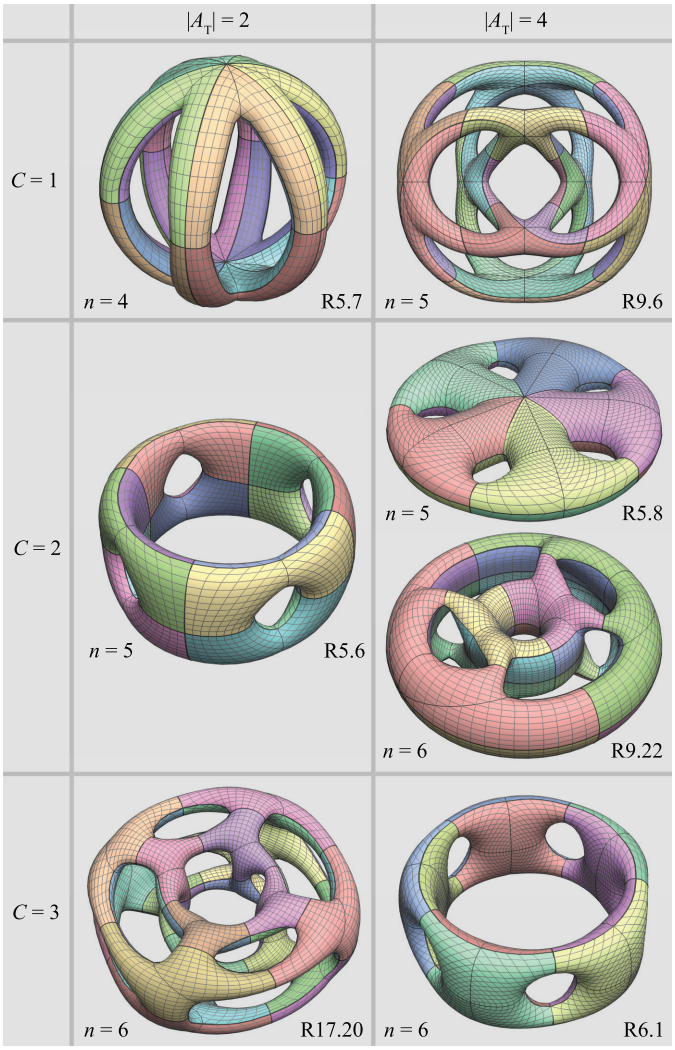

Fig. 9. Examples of face-transitive maps on surfaces that were used to depict regular maps. Various combinations of the number of triangles merged ($|A_T|$) and the number of chopped base points (C) are shown. The resulting number of base points n depends on the original number of base points, which depends on the configuration of the triangles.

desired, but more flexibility would be needed for a tube-like appearance.

The vertices of the boundaries are matched and placed back on the original surface. Optionally, the vertices at a user defined distance from the edges can be displaced inward also, to obtain a circular cross-section of the surface locally. To obtain a smoother surface, we apply 10-30 Laplacian smoothing steps, replacing vertices with the average of their neighbors. Compared to our earlier work, the meshes that result seem smoother, especially when many tubular shapes meet. Figure 8 shows examples of surfaces that can be used for the running case of regular map R5.6.

Figure 9 shows more examples of target surfaces to visualize regular maps (see Section 8). The simplest case is obtained by merging two triangles, and chopping the *M* or *N* point, the approach we used earlier. A target surface for R5.7 is shown as an example. The chopping of the *O* point; merging more than two triangles; and chopping multiple sets of fixed points gives a richer set of target shapes. For instance, the removal of points along the equator of a hosohedron, as well as the points at the top and/or bottom, enables us to model disks with a circular pattern of holes, possibly with a hole in the middle.

6 Alignment

It seems that we are close to done now. Given a regular map, we know how to factorize this as $H_S A_S$; we know how to produce a variety of target surfaces and how to factorize these as $H_T A_T$; for a proper match the groups H_S and H_T should be equal, as well as their fundamental regions, characterized by their Fuchsian signatures. However, just mapping the pattern of a fundamental region of the regular map to its counterpart on the target surface does not give a proper result: using Séquin's terminology [21], the map is only locally regular, and not globally regular. If both the source and target were infinite tilings, the map would be globally regular, however, we have to take the wrapping of faces across the boundaries of the plane model of the regular map into account. Hence, we have to carefully select fundamental regions on the regular map to obtain a good result. Figure 10 shows a suitable choice for the running case R5.6. The fundamental region of the target surface is shown black, and it obviously does not align with the tiles of the regular map, colored the same as in Figure 2.

We use a similar approach as in our earlier work [24], but instead of using fundamental regions with a uniform shape (quarter-tubes), we allow for more flexibility and therefore have to generalize.

6.1 Procedure

We first describe the problem in more detail. Suppose we want to visualize some regular map, and that we have a target surface with matching genus, group, and Fuchsian signature. Furthermore, assume we have chosen a fundamental region for this target surface, according to the requirements given in Section 5. Schematically, we can describe this fundamental region as a polygon with vertices $V_i, i = 1,\ldots,m$ (see Figure 4 for an example, where we just show the indices of the vertices). These vertices are fixed elliptic points on the target surface, which are partitioned into n fixed point sets $P_k^T, k = 1,\ldots,n$, using T as superscript to distinguish these target sets from the fixed point sets of the source regular map. Each of those sets has an associated order m_k^T.

Let L_i denote the label of the set to which V_i belongs, *i.e.*, $V_i \in P_{L_i}^T$. We call the first vertex V_i for which $L_i = k$ a base point B_k for the conjugate point set P_k^T, and consider other vertices with the same label as conjugate points of this base point. As all sets of conjugate points must be represented in a fundamental region, this gives us n such base points. The next task is to align these base points with fixed points of the regular map in hyperbolic space, thereby projecting the target surface back to the regular map.

Also for the regular map we have selected a fundamental region, which we use in combination with the generators of H_S to produce n sets of conjugate points $P_k^S, k = 1,\ldots,n$, with associated orders m_k^S. We do not constrain these points to lie at the plane model of the regular map, but also allow for a limited number of points outside, as the projected target region might not overlap with this plane model.

We use a depth first algorithm with backtracking to search for solutions. For the first point B_1, we select the first element of the first set P_k^S for which $m_1^T = m_k^S$. Next, we select B_2, discarding point sets P_k^S for which already a base point has been selected. If one of the tests applied fails, we select the next point from the current set P_k^S, and backtrack if all points of a set are exhausted. We do not take the ordering of the sets P^T and P^S into account, for instance if $m_1^T = 2$, then ultimately all elements of all sets P_k^S for which $m_k^S = 2$ can be considered as candidate points for the projection of B_1.

6.2 Tests

During the execution of this algorithm, a number of tests are applied on the geometry and group structure of the result. Assume that the fundamental region of the target has been projected to hyperbolic space. Let an edge e_i be defined as the edge between V_i and V_{i+1} (assuming $n + i = i$). There exists a geometric transformation M_i of this fundamental region to map an edge e_i to another edge e_j. Given the labels L_i of the vertices, this other edge is easy to determine: the two relations to be satisfied are $L_i = L_{j+1}$ and $L_{i+1} = L_j$. Obviously, $M_j = M_i^{-1}$.

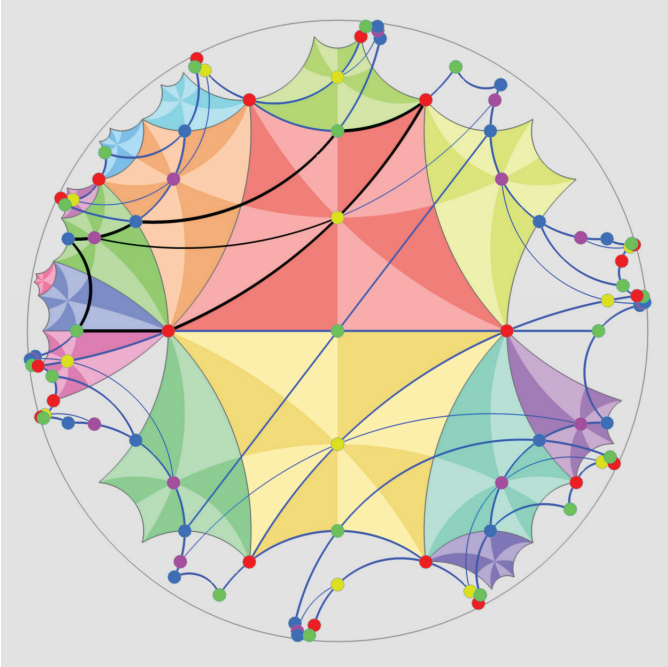

Fig. 10. The target map of the shapes shown in Figure 8 is aligned with plane model of R5.6. One fundamental region is indicated (black), as well as conjugate copies (blue). Thin lines show that the faces consist of pairs of chopped triangles. Unique colors are used to show the faces of the regular map, the triangles of the underlying triangle group are shown using a light-dark modulation.

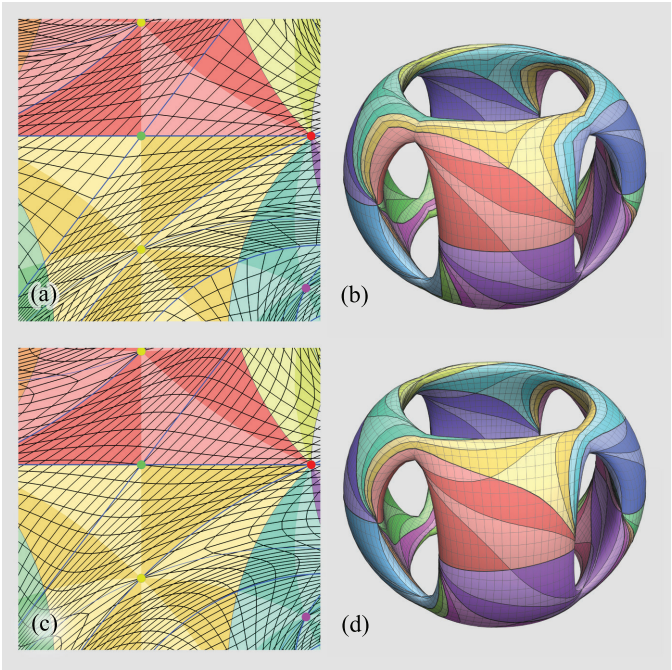

Fig. 11. Mapping R5.6 from hyperbolic space (Figure 10) to the target surface in 3D (Figure 8). (a) The chopped and aligned triangles of the target surface are meshed in the hyperbolic plane. (b) The mesh faces are clipped with the edges of the regular map, and the result is transferred to 3D. This works, but the edges of the regular map have sharp kinks, see for instance the edges bounding light and darker yellow areas. (c) This can be remedied by smoothing the target mesh first in the hyperbolic plane, (d) which gives a space model with much smoother edges of the regular map. Note that the close-ups of the hyperbolic plane cannot be directly traced back to the space models.

Furthermore, we can associate with each base point B_i a counterclockwise rotation R_i over $2\pi/m_i^T$. These rotations and edge mappings are related, which we can use to build up the projected fundamental region and perform checks.

If we look at the example shown in Figure 4, we see that $R_1 = M_1$: the rotation around vertex V_1 maps e_1 to e_8, and V_2 to V_8. For the next point B_2, we see that M_2 also maps V_2 to V_8, and application of M_8 maps it back to its original position. If we apply the same transformations to the fundamental region, we see that the effect of these mappings is the rotation R_2, *i.e.*, $R_2 = M_2M_8 = M_2M_1^{-1}$. This pattern holds in general. Application of M_i to B_i maps it to a vertex V_j, applying M_j in turn and repeating this step until the vertex is mapped back to the original point gives a sequence of transformations $M_iM_j\ldots$, which is equal to the rotation R_i.

We can use this by maintaining a list of n of these relations, and solving for an unknown transformation as soon as all but one of the transformations in a relation have been selected or computed. Furthermore, we see that $R_4 = M_4M_3^{-1}$ and $R_5 = M_4^{-1}$. Hence, the last point V_5 is fixed when V_4 has been selected, and if no point from the last remaining set P_k^S that matches with V_5 can be found, backtracking is required. Also, we can eliminate the mappings M_i from the list of equations, to obtain a single equation in the rotations R_i.

Furthermore, we require the projected fundamental region to be hyperbolically convex. The edges computed during the generation of the projected target map can be used as a clipping area for possible candidate points.

Besides the geometry, we also check for alignment of the source and target groups. A rotation around a base point B_i can be expressed as a word w_i in the target group and as v_i in the source group. Before the alignment procedure, we calculate the orders of words of the form $w_1w_2, w_1w_3, w_2w_3, w_1w_2w_3, w_1w_4, \ldots$. During the addition of new candidate points, we evaluate the orders of the corresponding words $v_1v_2, v_1v_3, v_2v_3, v_1v_2v_3, v_1v_4, \ldots$, and check if these orders match with the target results. If not, the new candidate is rejected, and the search is continued.

7 Mapping

The last step to obtain a space model is the projection of the pattern of the regular map to the faces of the target surface, and the transfer of this result to the target surface embedded in 3D. We use a similar approach as in our earlier work [24], but with some refinements. We use only the projected fundamental domain of the target surface, project the pattern of the regular map on this, and map this result to all copies of the fundamental domain on the surface, taking care that the labels of the regular map are properly adapted for the different copies.

The first step is to produce a mesh in the hyperbolic plane for the fundamental domain that is equivalent with the mesh used for the 3D version (see Figure 11(a)). To this end, per chopped triangle of the fundamental domain we use hyperbolic lines between vertices, which we regularly sample to yield boundary points. Next, points at opposite edges are connected by lines and sampled again, yielding a mesh. Transfer of the regular map to this mesh is done by clipping this mesh with the edges of the regular map. This is not trivial, as many cells are crossed by many lines, and also because all kind of special cases can and do occur. Rather than trying to elaborate all special cases, in the end we used a simple but more robust approach here. We pick a point in the interior of a triangle Δ of the mesh; determine in which triangle Δ_S of the regular map this point is located; split Δ if one the vertices of Δ_S is located inside or when edges cross, and recurse; otherwise Δ is stored.

Furthermore, some bookkeeping has to be done to maintain the status of vertices, faces, and edges for rendering faces and lines with the appropriate colors. All calculations are done in hyperbolic space, using the Poincaré disk model. An alternative is to use the Klein model here, like Razafindrazaka [16] has done, which is faster because hyperbolic lines are straight lines instead of circles. However, we found the overall performance to be acceptable for interactive use. Dependent

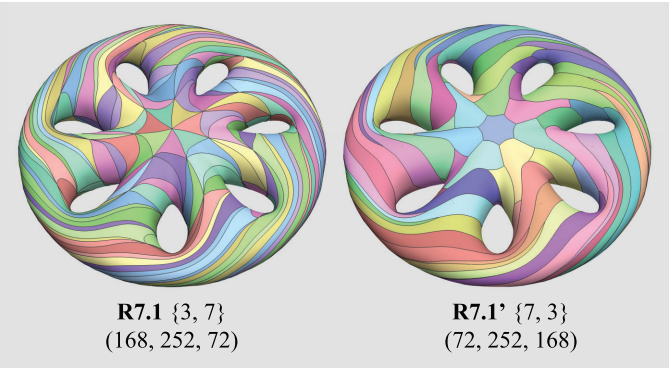

Fig. 12. Regular map R7.1: Visualization of the genus 7 Hurwitz surface

on the resolution of the meshes used, producing mappings typically takes 0.1 to 5s.

The result is shown in Figure 11(b). We see that just like in some images of our earlier work, edges of regular maps are not depicted smoothly, but exhibit strange kinks, for instance in the edges separating light and dark yellow areas. Here this might be acceptable, in other cases the results can be much worse. The kinks are due to discontinuities in the direction of mesh-lines across boundaries in the hyperbolic plane. Higher resolution meshes or smoothing the surface in 3D do not remedy this, just like in computer graphics acting on a surface to correct a poor texture map makes no sense.

Fortunately, we found that a much better result can be obtained by smoothing the meshes in the hyperbolic plane before the mapping is done (see Figure 11(c) and (d)). We do this for the mesh of the fundamental region of the target surface, using iterative Laplacian smoothing, with periodic boundary conditions. We keep the rotational points fixed, for the other points we replace these per step by the average of their four direct neighbors. If a point is located at the boundary, one or two neighboring points might be absent. For these we use virtual points, obtained by translating points in the mesh according to the transformation M_i described in the previous section.

8 Results

In this section we present results and discuss these. The approach described in the preceding sections leads to about 45 new space models of regular maps, counting duals separately. Also, the earlier space models directly derived from genus 0 and 1 surfaces are reproduced, but not the models derived recursively from higher genus surfaces. The latter should be possible in principle also with this approach, but it is much harder to implement. The earlier tubification approach nicely exploits a simple homogenous intermediate representation (wireframe models), here such a representation does not pop up naturally.

Figure 13 shows 25 examples of results. From top to bottom, these are sorted for target surface used (first two rows: hosohedra; third row: Platonic solids; last two rows: tori); from left to right for genus. Séquin [21] already had found a somewhat complex solution for R4.2 $\{4, 5\}$ (after observing that the use of a disk with four symmetric holes does not work out), the solution shown in Figure 13 is simpler. In these figures we typically use 4-6 different colors, using subgroups of the group of the regular map to decide upon which color to use for what face. When all faces are colored differently, they are hard to distinguish. However, some regular maps, such as R7.1, do not have subgroups such that only a limited number of colors can be used, and for this 28 colors and 35 for its dual had to be used.

Six new regular maps based on Platonic solids were found: R9.16, R19.3, R29.10 and their duals. The surface used for R9.16 is the result of chopping face and edge points of a double-walled tetrahedron. The space models of R29.10 and its dual are obtained by chopping edge points of a double-walled icosahedron. Also, they can be considered as a tubified rhombic triacontahedron. The surfaces are uniformly covered with starfish-like shapes, with three (R29.10) bent legs (forming a triskele) or five (R9.10') zig-zag legs. Each leg here folds around seven tubes before reaching its endpoint.

Figure 12 shows a space model of the genus 7 Hurwitz surface, also known as the MacBeath surface. In Section 2 we mentioned Hurwitz surfaces. Such surfaces with a maximal number of symmetries are rare, the first few cases are obtained for $g = 3, 7, 14$, and 118. The Hurwitz surface for genus 3 is regular map R3.1, R7.1 is the next one. The associated group of automorphisms is $PSL(2, 8)$. Séquin has spent much effort to find space models for this regular map, and made drawings what these could look like, using a 2D disk model [23]. These results confirm his findings, and are the first digital model and 3D visualization of R7.1.

Images of this surface were distributed among a number of experts in geometry (including Marston Conder, Jörg Wills, and Jürgen Bokowski), and they were all excited. The study of regular maps is an active area in mathematics, and finding a polyhedral version (with flat triangles and without self-intersections) of this surface has been a long standing research problem and it is still open. This visualization is not polyhedral, but it does provide insight why such a polyhedral realization might not exist, as many long curve segments go around the rim of the shape.

These results show that our approach is more generic than our earlier work, and as a result, the number of regular maps that can be visualized almost doubles. Furthermore, the resulting images are smoother, thanks to the smoothing of the mesh in the hyperbolic plane.

Still, there is work to be done, and we hoped that many more results would have come out. The alignment phase is critical here, for many cases we found matching source regular maps and target surfaces, with compatible groups and Fuchsian signatures, but the algorithm was not able to find suitable alignments. For instance, there is a match between R14.1, the next Hurwitz surface, and a 13-hosohedron, with D_{26} as group and (0; 2, 2, 2, 2, 2, 2) as Fuchsian signature. This suggests that R14.1 can be mapped on a ring with 13 holes, but no solution was found. The causes for this are unclear yet. It might be that the restrictions we put on fundamental regions (see Section 5) are too constraining, also, there might be other implicit assumptions (and flaws) in our implementation. The chase is not over yet.

Another area where improvements can be made is the visual representation. Static images fall short to fully understand the structure of the more complex cases, and also with animation (see accompanying video) and interactive viewing it is still often difficult to understand what is going on. The use of physical models, made by 3D printing, will lead to results that are easier to understand. However, we think this complexity is an important part of the charm of these objects, *i.e.*, the fact that very compact definitions of highly symmetric and regular structures can lead to shapes with a wild complexity that is not easy to grasp at first sight.

9 Conclusion

We have presented a generalization of our earlier approach to visualize regular maps. The key idea is to factorize regular maps and target surfaces, to find matchings between their shape and structure. A broad class of target surfaces could be defined based on the process of duplicating surfaces, merging triangles, punching holes, and gluing edges. The use of concepts from group theory was highly useful to provide a solid grounding as well as for implementation. As a result, about 45 new space models for new regular maps could be found, including for the genus 7 Hurwitz surface; but there are still many cases waiting for solutions.

We hope that these results are useful, not only for mathematicians, but also for a broader audience, for purposes such as education (as concrete examples of abstract concepts), entertainment (trying to understand the structure and solving new cases), and artistic use.

Acknowledgments

I thank Carlo Séquin for his expert feedback on an earlier version of this article and the many inspiring discussions we had, and Arjeh Cohen for his challenge to visualize Hurwitz surfaces.

Fig. 13. Results. R$g.i$: regular map using Conder's notation, g: genus; $\{p, q\}$: polygons have p edges, at vertices q edges meet; (F, E, V): number of faces, edges, and vertices.

REFERENCES

[1] J. W. Anderson. *Hyperbolic Geometry, 2nd edition*. Springer, 2007.

[2] A. F. Beardon. *The Geometry of Discrete Groups*. Springer, 1983.

[3] J. Bokowski and J. Wills. Regular polyhedra with hidden symmetries. *The Mathematical Intelligencer*, 10(4):27–32, 1988.

[4] M. Conder. Orientable regular maps of genus 2 to 101, 2006. `http://www.math.auckland.ac.nz/~conder`.

[5] M. Conder and P. Dobcsányi. Determination of all regular maps of small genus. *Journal of Combinatorial Theory, Series B*, 81:224–242, 2001.

[6] H. Coxeter. *Introduction to Geometry, Second Edition*. Wiley, 1989.

[7] H. Coxeter and W. Moser. *Generators and Relations for Discrete Groups*. Springer-Verlag, Berlin, 1984. Reprint of the fourth edition.

[8] D. Dunham. 168 butterflies on a polyhedron of genus 3. In *Proc. BRIDGES 2002 Conference, Baltimore*, pages 197–204, 2002.

[9] P. A. Firby and C. F. Gardiner. *Surface topology, 3rd edition*. Horwood publishing, 2001.

[10] The GAP Group. *GAP – Groups, Algorithms, and Programming, Version 4.7.4*, 2014.

[11] A. Hurwitz. Ueber algebraische Gebilde mit eindeutingen Transformationen unter sich. *Math. Ann.*, 41:403–442, 1893.

[12] S. Katok. *Fuchsian Groups*. University of Chicago Press, 1992.

[13] S. Levy, editor. *The Eightfold Way: The Beauty of Klein's quartic curve*. Cambridge University Press, 2001.

[14] R. Nedela. Regular maps – combinatorial objects relating different fields of mathematics. *Journal of the Korean Mathematical Society*, 38(5):1069–1105, 2001.

[15] H. Poincaré. Théorie des groupes Fuchsiens. *Acta Mathematica*, 1:1–62, 1882.

[16] F. Razafindrazaka. Visualization of high genus regular maps. Master's thesis, Freie Universität Berlin, 2012.

[17] F. Razafindrazaka and K. Polthier. The 6-ring. In *Proc. BRIDGES 2013 Conference, Enschede*, pages 197–204, 2013.

[18] P. Scholl, A. Schürmann, and J. Wills. Polyhedral models of Felix Klein's group. *The Mathematical Intelligencer*, 24(3):37–42, 2002.

[19] E. Schulte and J. Wills. A polyhedral realization of Felix Klein's map $3,7_8$ on a Riemann surface of genus 3. *J. London Math. Soc.*, 32:539–547, 1985.

[20] C. H. Séquin. Patterns on the genus-3 Klein quartic. In *Proc. BRIDGES 2006 Conference, London*, pages 245–254, Aug. 2006.

[21] C. H. Séquin. Symmetric embedding of locally regular hyperbolic tilings. In *Proc. BRIDGES 2007 Conference, San Sebastian*, pages 379–388, Aug. 2007.

[22] C. H. Séquin. My search for symmetrical embeddings of regular maps. In *Proc. BRIDGES 2010 Conference, Pécs*, pages 85–94, July 2010.

[23] C. H. Séquin. Personal communication, 2012.

[24] J. J. van Wijk. Symmetric tiling of closed surfaces: Visualization of regular maps. *ACM Transactions on Graphics*, 28(3):12 pages, 2009.